

## Second Virial Coefficients Revisited. 5. Generalization of the Concept of Intramolecular Contributions to Low Molecular Weight Polymers

H. Geerissen,<sup>†</sup> P. Schützeichel,<sup>‡</sup> and B. A. Wolf\*

*Institut für Physikalische Chemie der Universität Mainz, Jakob-Welder-Weg 13, D-6500 Mainz, Germany*

*Received January 9, 1990; Revised Manuscript Received June 8, 1990*

**ABSTRACT:** In the preceding papers of this series, it has been shown theoretically and experimentally how the Flory-Huggins interaction parameter  $\chi$  and the Huggins coefficient  $k_H$  for polymers differing in molecular weight can be built up from the contributions of inter- and intramolecular contacts between polymer segments. The present work reports on measurements with the system isooctane/polyisobutylene ( $M$  ranging from 5 to 1350 kg/mol) particularly performed to extend the molecular weight range to lower values. The evaluation of the obtained data according to the equations following from the concept of intramolecular contributions yields two intersecting straight lines instead of one, for  $A_2$  as well as for  $k_H$ : In the lower molecular weight region the measured values become up to twice as large as that predicted theoretically. It is demonstrated that the reason for this behavior lies in the fact that *triples of segments* become important upon the reduction of the molecular weight, even if the polymer concentration remains so low that it is only necessary to consider *pairs of polymer molecules*. Taking this feature into consideration, we formulate a generalized theoretical equation that is able to describe the observed behavior in the entire range of molecular weights.

### Introduction

As polymer solutions are diluted by the addition of solvent, the macromolecules can be separated indefinitely, but this is not true for the polymer segments from which they are made up. In the concentration range of pair interaction between the solute this situation leads to the coexistence of large volume elements that are totally free of segments with the domains of the polymer coils, within which the volume fraction of segments is normally low but cannot be reduced below a characteristic limiting value. This situation makes the theoretical discussion of pair interaction, like the second osmotic virial coefficient  $A_2$  or the Huggins parameter  $k_H$ , for macromolecular chains rather complicated. The most widespread attempts to describe the molecular weight dependence of  $A_2$  and  $k_H$  are based on the fact that segments belonging to one molecule can influence the placement of those stemming from another one. These excluded-volume theories have, however, become so complicated in the course of their adjustment to experimental findings that an entirely different approach, accounting for the above situation in a different way, appeared worthwhile.

The central starting point of this procedure is the change of coil dimension with composition (equivalent to the lowered or enhanced probability of placement of alien segments within the overlap region of two polymer coils). As a consequence of this change in size, intramolecular contacts between segments are opened ( $A_2 > 0$ ) in addition to intermolecular ones as solvent is added; this means that the measured virial coefficients also contain intramolecular contributions. For the description of the influence of molecular weight it is assumed that (i) these two types of contacts are thermodynamically and rheologically unequal and (ii) that the ratio of their numbers depends on  $M$ . The justification of hypothesis i becomes very obvious in the case of the entropy of dilution (one constituent of  $A_2$ ): As a solvent molecule is inserted to open a contact between two segments belonging to different

molecules, it contributes to the total and eventually infinite separation of the polymer pair. In contrast to that, the opening of an intramolecular contact has only little effect on the gain in entropy, since these segments can only be separated to a maximum extent determined by their relative position on the chain. The feasibility of assumption ii can be seen from the fact that only the intermolecular contacts survive as the molecular weight is sufficiently lowered.

In the preceding papers of this series it was demonstrated how experimental data concerning  $A_2(M)$  and  $k_H(M)$  (different polymers and highest possible variation of solvent power) can be described quantitatively by the theoretical equations following from this concept. The present contribution reports on new measurements that, for the first time, also include low molecular weight polymers and that reveal new phenomena in this area. Furthermore, it demonstrates which generalization of the theoretical relations is required to make the approach applicable in the entire range of molecular weights.

### Materials and Procedures

**Materials.** The solvents used for fractionation, characterization, and physicochemical measurements are summarized in Table I, together with their producers, purity grades, and abbreviations.

The polymers were fractionated from industrial polyisobutylenes (Oppanol B10, B15, and B50 and the product DS 3303 from BASF Ludwigshafen, Germany). Parts of the samples used were obtained from CPF (continuous polymer fractionation) experiments as described earlier.<sup>5,6</sup> To obtain additional fractions numerous discontinuous preparative experiments were also carried out.  $M_w$  values, molecular nonuniformities  $U = M_w/M_n - 1$ , and fractionation procedures are collected in Table II. The capital letter of the abbreviations given in the last column states whether the particular fraction constitutes a gel (G) or a sol (S), and the small superscripts recall their history. <sup>50</sup>G, for instance, means that the material is the gel of the third fractionation step, which in turn has been produced from the gel of the second, itself being the sol of the first. The figures in the sample abbreviation indicate their rounded molecular weights in kg/mol.

**Gel Permeation Chromatography.** To determine the non-uniformity of the samples, GPC measurements were carried out. The experimental details were already described.<sup>5</sup>

<sup>†</sup> Present address: Kächele-Cama Latex GmbH, D-6405 Eichenzell, Germany.

<sup>‡</sup> Present address: KGW KG, D-5466 Neustadt/Wied, Germany.

Table I  
List of Solvents

solvent	abbrev	producer, purity	use
toluene	TOL	Merck, reinst. >99%	solvent for fractionation
2-butanone	MEK	Merck, reinst. >99%	nonsolvent for fractionation
methanol		Merck, reinst. >99.5%	nonsolvent for fractionation
isooctane	IO	Merck, p.a., >99.5%	light scattering, intrinsic viscosity
tetrahydrofuran	THF	BASF, rein, distillation by circulation over K	GPC measurements
benzene		Merck, p.a., >99.7%, distillation	light scattering (calibration)

Table II  
List of Polymers<sup>a</sup>

sample	$M_w$	$U = \frac{M_w}{M_n} - 1$	fractionation procedure	form <sup>b</sup>
PIB 5	5	0.25	DS 3303; FP with TOL/MEK-methanol	GS
PIB 6	6.2	0.25	DS 3303; FP with TOL/MEK	GS
PIB 9	8.9	0.25	B10; FP with TOL/MEK	SSS
PIB 12	11.8	0.17	DS 3303; FP with TOL/MEK	GG
PIB 16	15.8	0.17	B10; FP with TOL/MEK	SSG
PIB 23	22.9	0.16	B15; FP with TOL/MEK	SSSSS
PIB 26	26.1	0.10	B10; FP with TOL/MEK	SGG
PIB 34	33.9	0.15	B10; FP with TOL/MEK	GS
PIB 39	39.0	0.15	B15; FP with TOL/MEK	SSSG
PIB 56	56.4	0.13	B10; FP with TOL/MEK	SSG
PIB 61	61.4	0.14	B15; FP with TOL/MEK	SSSGS
PIB 80	80.5	0.23	B15; FP with TOL/MEK	SSSGG
PIB 87	87.0	0.24	B15; CPF (cf. ref 6, Sol IV)	SSG
PIB 95	95.0	0.23	B15; FP with TOL/MEK	SSG
PIB 120	122	0.20	B50/Sol II (cf. ref 5); FP with TOL/MEK	SGS
PIB 140	140	0.25	B15; CPF (cf. ref 6, Gel IV)	
PIB 180	180	0.29	B15; CPF (cf. ref 6, Sol III)	
PIB 230	230	0.19	B50/Sol III (cf. ref 5); FP with TOL/MEK	SG
PIB 270	270	0.30	B15 (cf. ref 6, Gel III)	
PIB 390	393	0.19	B50/Sol IV (cf. ref 5); FP with TOL/MEK	SS
PIB 610	612	0.24	B50/Gel IV (cf. ref 5); FP with TOL/MEK	SG
PIB 830	832	0.25	B50/Gel IV (cf. ref 5); FP with TOL/MEK	SS
PIB 1100	1100	0.30	B50 (cf. ref 5, Gel IV)	
PIB 1360	1360	0.25	B50/Gel IV (cf. ref 5); FP with TOL/MEK	GGG

<sup>a</sup> FP = fractionation by precipitation; CPF = continuous polymer fractionation. <sup>b</sup> S = sol; G = gel. Superscripts indicate history of fractionation. See Materials and Procedures for additional details.

**Refractive Index Increments.** Since this quantity appears as a squared term in the light scattering equation, it must be determined very accurately. Values of  $dn/dc$  reported in the literature<sup>7</sup> are based on measurements with high molecular weight material. Since the present study deals with molecular weight influences, it turned out necessary to check the  $M$  dependence of the refractive index increment. This was done for five samples (PIB 5, 9, 16, 34, and 230) on an instrument described in the literature<sup>8</sup> after calibration with potassium chloride, using the procedure and data given in reference 9.

**Light Scattering.** All experiments were performed on the commercially available instrument Fica 50 (Sofica, France) in isooctane at 25 °C with vertically polarized light of 546 nm. The calibration was carried out with freshly distilled benzene. For each sample of PIB five different concentrations were measured after filtration (Sartorius 0.45- $\mu$ m filters). The evaluation of primary data was performed as usual.<sup>9</sup>

**Viscometry.** The capillary instrument AVS 300 of Schott-Geräte (Hofheim, Germany) was used with a capillary diameter of 0.54 mm; when necessary, running times were corrected according to Hagenbach. Five solutions were, as a rule, measured for each polymer sample at 20, 30, and 40 °C; the filtration was performed as in the case of the light scattering experiments.

## Results

**Refractive Index Increment.**  $\Delta n$ , the difference of

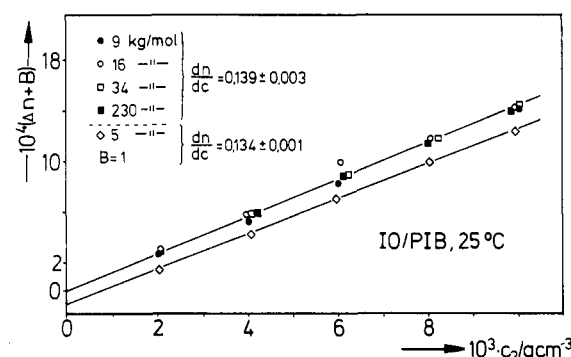


Figure 1. Dependence of  $\Delta n$  (the difference of the refractive index of solutions of PIB and that of the pure solvent IO) on polymer concentration  $c_2$  for 25 °C. The samples used and the refractive index increments obtained for the high molecular weight samples and PIB 5, respectively, are indicated in the graph.

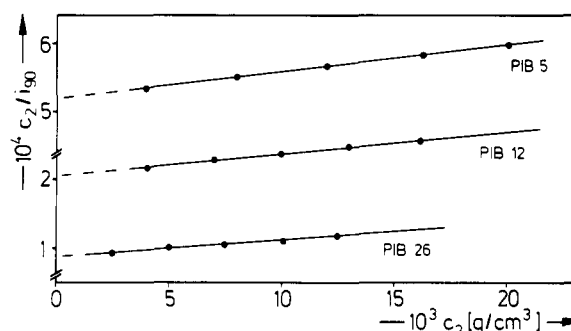


Figure 2.  $c_2/i_{90}$  as a function of  $c_2$  for solutions of the indicated samples of PIB in IO at 25 °C;  $i_{90}$  is the galvanometer reading for the solution at an angle at 90° minus that for the pure solvent, and  $c_2$  is the polymer concentration in g/cm<sup>3</sup>.

the refractive index of the solutions of PIB and that of the pure solvent, is shown in Figure 1 as a function of the polymer concentration  $c$  for five different samples and 25 °C;  $dn/dc = 0.139 \pm 0.025$  cm<sup>3</sup>/g, independent of  $M$  for  $9 < M$  (kg/mol)  $< 230$ , so that this value is in the following used for PIB of molecular weights larger than 9 kg/mol. For the shorter chains of PIB 5,  $dn/dc = 0.134 \pm 0.010$  cm<sup>3</sup>/g.

**Light Scattering.** Figure 2 shows examples for the determination of  $M_w$  values and of second osmotic virial coefficients  $A_2$  in the case of low molecular weight samples of PIB. The Zimm plot of Figure 3 is typical for the results with high molecular weight material, for which  $\langle R_z^2 \rangle^{0.5}$ , the  $z$ -average radii of gyration, were also determined. All experimental data are collected in Table III.

**Viscometry.** To determine intrinsic viscosities  $[\eta]$  and Huggins coefficients  $k_H$ , the reduced viscosities  $\eta_{red} = (\eta - \eta_0)/(\eta_0 c)$  were extrapolated to infinite dilution as shown in the example of Figure 4. For the calculation of  $c$ , the change of density of the solutions resulting from the polymer and the influences of temperature were taken into account. The obtained data are collected in Table IV together with results from previous measurements.<sup>3</sup>

**Viscosity-Molecular Weight Relationships.** The  $[\eta]$  and  $M$  values collected in Tables IV and II are evaluated

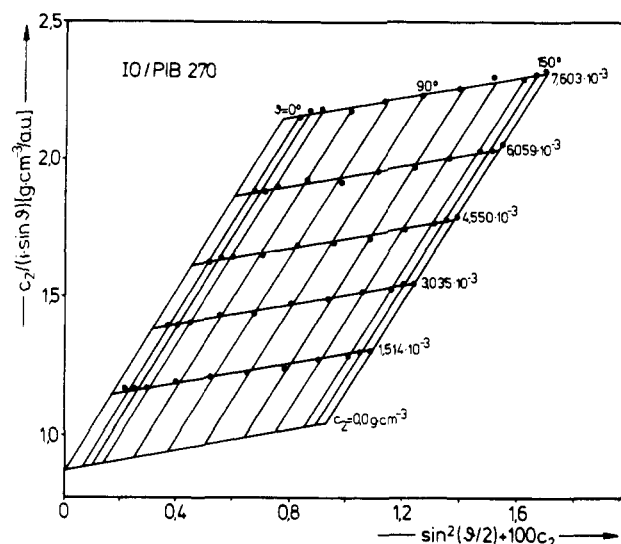


**Figure 3.**  $c_2/(i \sin \theta)$  as a function of  $\sin^2(\theta/2) + 100c_2$  (modified Zimm plot) for the system IO/PIB 270 and 25 °C;  $i$  is the galvanometer reading for the solution at the angle of  $\theta$  minus that for the pure solvent, and  $c_2$  is the polymer concentration in  $\text{g}/\text{cm}^3$ .

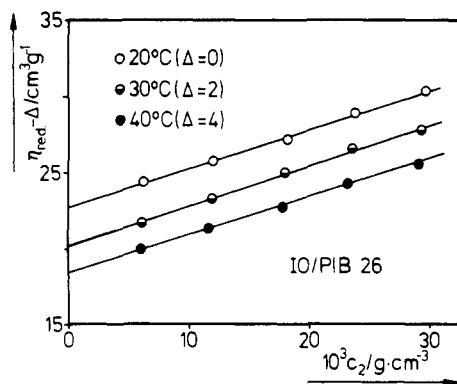


**Figure 4.** Reduced viscosity  $\eta_{\text{red}} = (\eta - \eta_0)/(\eta_0 c_2)$  as a function of polymer concentration  $c_2$  (Huggins plot) for the system IO/PIB 26 at the indicated temperatures.

in Figure 5 according to the Kuhn–Mark–Houwink equation. The resulting parameters can be read from Table V; within the limited temperature range under investigation they can be considered constant. The somewhat smaller exponents of the present relation as compared with that reported previously<sup>3</sup> results from the extension of the molecular weight range toward lower  $M$  values.

## Discussion

**Theoretical Background.** Calculations concerning the molecular weight dependence of pair interactions in terms of the excluded-volume theory are comparatively complicated and often at variance with experiments.<sup>4</sup> For this reason a totally different concept has been developed and tested during the past years.<sup>2–4</sup> It accounts for the fact that coil dimensions change with varying polymer concentration. In the good solvent of present interest, the polymer coil dimensions increase as solvent is added until a characteristic maximum expansion, depending on the value of  $M$ , is reached in the infinitely dilute state. As a consequence of this situation not only intermolecular contacts between segments belonging to different chains are opened upon the addition of solvent but also some intramolecular ones. Postulating that the effects  $\epsilon^{(i)}$  and  $\epsilon^{(o)}$  associated with such an insertion of the solvent molecule between two segments differ from each other in the general

**Table III**  
Light Scattering Data for the System IO/PIB at 25 °C

sample	$10^4 A_2/(\text{cm}^3 \text{ mol g}^{-2})$	$\langle R_z^2 \rangle^{1/2}/\text{\AA}$
PIB 5	7.96	
PIB 6	8.03	
PIB 9	6.9	
PIB 12	6.61	
PIB 16	6.2	
PIB 23	5.56	
PIB 26	5.30	
PIB 34	5.00	
PIB 39	4.76	
PIB 56	4.42	
PIB 61	4.23	
PIB 80	4.09	118
PIB 87	3.93	128
PIB 95	4.08	104
PIB 120	3.84	140
PIB 140	3.72	187
PIB 180	3.67	217
PIB 230	3.57	193
PIB 270	3.51	247
PIB 390	3.34	231
PIB 610	3.15	352
PIB 830	3.14	404
PIB 1100	3.00	479
PIB 1360	2.94	545

**Table IV**  
Intrinsic Viscosities and Huggins Coefficients for the System IO/PIB at Different Temperatures

sample	$T/^\circ\text{C}$	$[\eta]/(\text{cm}^3 \text{ g}^{-1})$	$k_H$
PIB 5	20	8.34	1.018
	30	8.37	0.939
	40	8.29	0.920
PIB 9	20	12.28	0.683
	30	12.19	0.665
	40	12.08	0.668
PIB 16	20	16.84	0.597
	30	16.74	0.579
	40	16.63	0.569
PIB 26	20	22.66	0.501
	30	22.21	0.527
	40	22.47	0.480
PIB 34	20	26.86	0.496
	30	26.39	0.535
	40	26.72	0.473
PIB 56	20	35.40	0.504
	30	35.70	0.466
	40	35.87	0.445
PIB 120 <sup>a</sup>	20	56.50	0.430
	30	56.20	0.425
	40	55.91	0.422
PIB 230 <sup>a</sup>	20	84.16	0.447
	30	84.13	0.428
	40	83.67	0.423
PIB 390 <sup>a</sup>	20	116.8	0.430
	30	116.1	0.427
	40	115.1	0.435
PIB 610 <sup>a</sup>	20	157.5	0.377
	30	157.3	0.366
	40	156.7	0.361
PIB 830 <sup>a</sup>	20	187.1	0.430
	30	186.5	0.423
	40	185.5	0.422
PIB 1100 <sup>a</sup>	20	219.8	0.427
	30	218.8	0.422
	40	217.9	0.417

<sup>a</sup> The data for PIB 120 to PIB 1100 are taken from the literature.<sup>3</sup>

case, the observed variation of pair interaction parameters (such as the Flory–Huggins interaction parameter  $\chi$  or the Huggins coefficient  $k_H$ ) results from the change in the mixing ratios of  $\epsilon^{(i)}$  and  $\epsilon^{(o)}$  if  $M$  is varied. These ideas are expressed quantitatively<sup>4</sup> in eq 1

$$\epsilon = 0.5[\epsilon^{(i)} + \epsilon^{(o)}] + 0.5[\epsilon^{(i)} - \epsilon^{(o)}](K_0/K)M^{-(a-0.5)} \quad (1)$$

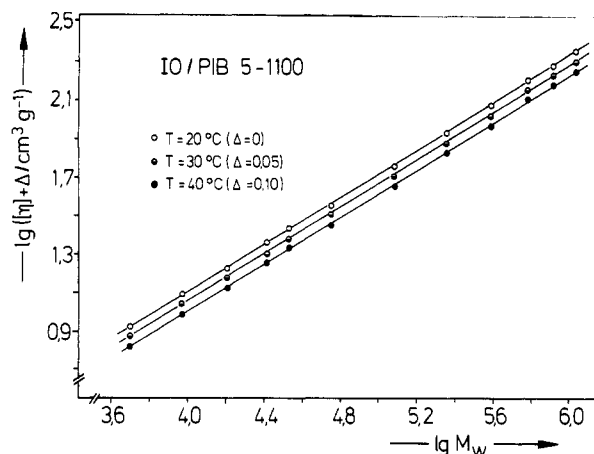


**Figure 5.** Intrinsic viscosities  $[\eta]$  as a function of  $M_w$  for the system IO/PIB at the indicated temperatures.

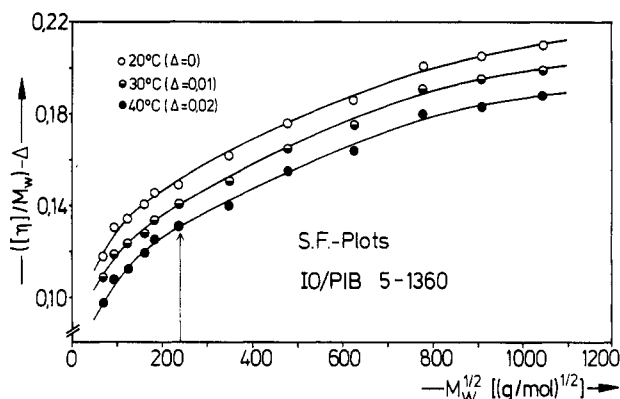


**Figure 6.** Stockmayer-Fixman plot (eq 7) for the system IO/PIB at the temperatures stated. The arrow indicates the location of the discontinuity in the evaluation shown in Figure 7.

**Table V**  
Parameters of the Kuhn-Mark-Houwink Equation  
 $[\eta] = KM_w^a$  of the System IO/PIB 5-1100 for Different Temperatures

$T/^\circ\text{C}$	$10^2 K/(\text{cm}^3/\text{g})$	$a$	$r$
20	4.814	0.606	0.99994
30	4.786	0.606	0.99994
40	4.847	0.605	0.99992
25	4.82	0.606	

**Table VI**  
Comparison of the  $K_\theta$  Values ( $\text{cm}^3 \text{g}^{-1}$ ) for PIB Obtained with IO from Stockmayer-Fixman Plots with That Measured in Different  $\theta$  Solvents

IO/25 °C		ethyl			
$M_w/(\text{kg/mol})$		heptanoate <sup>4</sup>			
5-34	34-610	$\theta = 34^\circ\text{C}$	benzene <sup>7</sup> $\theta = 24^\circ\text{C}$	phenetole <sup>7</sup> $\theta = 86^\circ\text{C}$	anisole <sup>7</sup> $\theta = 105^\circ\text{C}$
0.106	0.129	0.105	0.107	0.091	0.091

$K$  and  $a$  are the parameters of the Kuhn-Mark-Houwink equation

$$[\eta] = KM^a \quad (2)$$

where  $a$  becomes 0.5 and  $K = K_\theta$  at the  $\theta$  temperature.

If  $a$  and  $K$  are known for the system of interest and  $K_\theta$  is available from theoretical considerations or additional experiments, the measured variation of  $\epsilon$  with  $M$  can be used to determine the individual effects  $\epsilon^{(i)}$  and  $\epsilon^{(o)}$  for the opening of "outer" and "inner" intersegmental contacts. In the case of the thermodynamic interaction parameter  $\chi$ , the directly obtained  $A_2$  values must be converted by

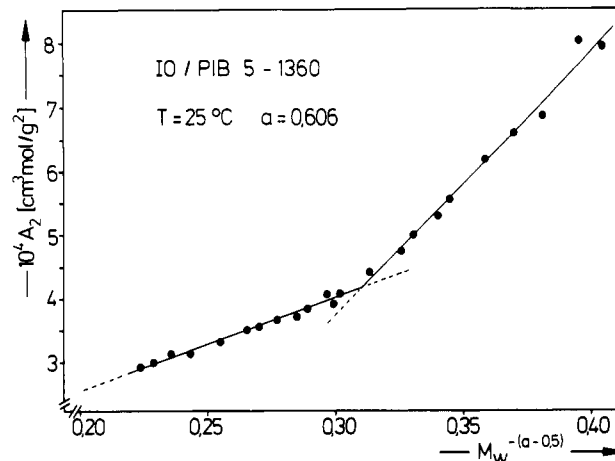


**Figure 7.** Evaluation of the molecular weight dependence of the second osmotic virial coefficient  $A_2$  according to eq 4 for the system IO/PIB at 25 °C;  $a$  is the exponent of the Kuhn-Mark-Houwink equation (2).

means of eq 3

$$A_2 = (0.5 - \chi)/(\rho^2 V_1) \quad (3)$$

in which  $\rho$  is the density of the polymer and  $V_1$  is the molar volume of the solvent. This leads to the following expression for the molecular weight dependence of  $A_2$ :

$$A_2 = A_2^\infty + bM^{-(a-0.5)} \quad (4)$$

The limiting value of  $A_2$  for infinitely large molecular weight is given by

$$A_2^\infty = 0.5(1 - [\chi^{(i)} + \chi^{(o)}]) / (\rho^2 V_1) \quad (5)$$

and  $b$  by

$$b = -0.5[\chi^{(i)} - \chi^{(o)}](K_\theta/K)/(\rho^2 V_1) \quad (6)$$

In the case of the hydrodynamic interaction parameter  $k_H$ , eq 1 can directly be applied. In both cases the evaluation is performed by plotting the molecular weight dependent data as a function of  $M^{-(a-0.5)}$ , the slope yielding the difference in the outer and inner effects and the intercept their sum.

**$K_\theta$  Values.** Since  $K_\theta$  depends on the chemical nature of the particular  $\theta$  solvent in some cases, we attempted to determine this parameter from the existing data for IO by means of the Stockmayer-Fixman equation.<sup>10</sup>

$$[\eta]/M_w^{0.5} = K_\theta + 0.51\Phi_0 BM_w^{0.5} \quad (7)$$

From Figure 6 it can be seen that the dependences are curved and that the above relation is only valid within certain limited ranges of  $M$ . Similar curves are also obtained in the evaluation according to Berry.<sup>11</sup>

In view of the discussion in the next paragraph,  $K_\theta$  values were calculated for the low ( $\leq 34$  kg/mol) and for the high molecular weight regime ( $\geq 34$ ) and compared with that reported for different  $\theta$  solvents. These data are collected in Table VI. The fact that the value resulting from the evaluation according to the Stockmayer-Fixman equation for the low molecular region is in good agreement with that reported for ethyl heptanoate<sup>4</sup> and benzene<sup>7</sup> is probably only accidental.

**Thermodynamic Pair Interaction.** The evaluation of the data collected in Table III according to eq 4 is shown in Figure 7. For the first time two straight lines, which intersect as  $M \approx 60$  kg/mol, are observed instead of one. This observation is, however, not at variance with earlier

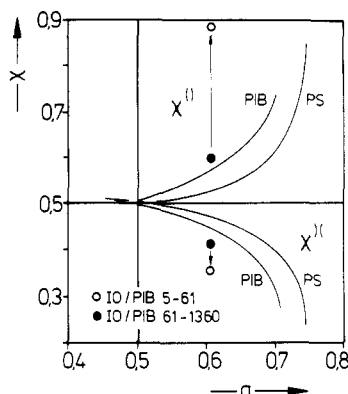


**Figure 8.** Flory-Huggins interaction parameters for the opening of inter- and intramolecular contacts between polymer segments,  $\chi^{(1)}$  and  $\chi^{(0)}$ , as a function of the exponent  $\alpha$  of the Kuhn-Mark-Houwink equation. The full lines represent the results from earlier measurements within the higher molecular weight region for solutions of PIB and polystyrene (PS) in different solvents. The full circles give the data calculated for the system IO/PIB from Figure 7 for  $M \geq 60$  kg/mol, and the empty ones for  $M \leq 60$  kg/mol.

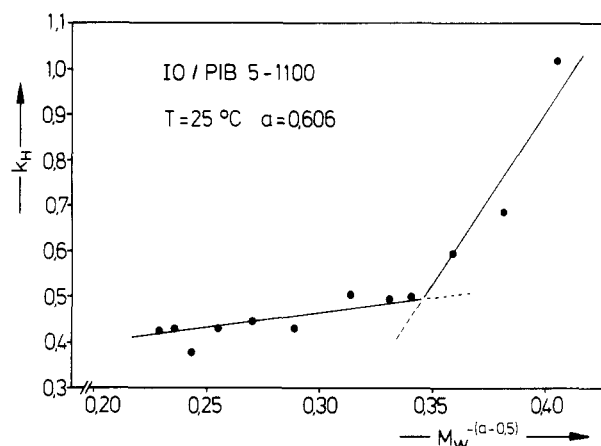


**Figure 9.** Evaluation of the molecular weight dependence of the Huggins coefficient  $k_H$  according to eq 1 ( $\epsilon = k_H$ ) for the system IO/PIB at 25 °C;  $\alpha$  is the exponent of the Kuhn-Mark-Houwink eq 2.

results since no measurements have so far been performed with a sufficiently large number of low molecular weight samples.

For the determination of  $\chi^{(1)}$  and  $\chi^{(0)}$  from Figure 7 by means of eqs 5 and 6 one requires  $K_\theta$ . No matter whether the data given in Table VI for  $\theta$  solvents are used for the evaluation or whether the calculation is performed on the basis of two different  $K_\theta$  values for the lower and higher molecular weight region, respectively, the results are practically identical: As can be seen from Figure 8, the effect for opening outer contacts is in both regimes of the same order of magnitude as that already reported,<sup>4</sup> whereas for the inner contacts this is only true inside the region of high molecular weights; as  $M$  falls below ca. 60 kg/mol,  $\chi^{(0)}$  assumes a value that is almost 50% larger.

**Viscometric Pair Interaction.** The evaluation of the viscosity data collected in Table IV according to eq 1 with  $\epsilon = k_H$  is shown in Figure 9. Although there are fewer data points and larger experimental uncertainties than in the case of  $A_2$ , one can again construct two straight lines that intersect at approximately the same  $M$  value.

For the determination of  $k_H^{(1)}$  and  $k_H^{(0)}$  from the slopes and intercepts of the two lines of Figure 9, the influence of the chosen  $K_\theta$  value is very little, similar to the situation described in the previous paragraph for  $\chi$ . As with the

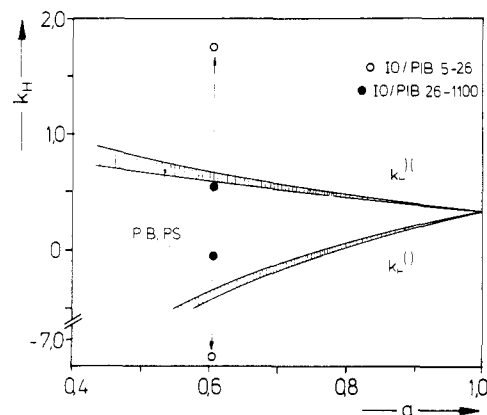


**Figure 10.** Huggins coefficients for the opening of inter- and of intramolecular contacts between polymer segments,  $k_H^{(1)}$  and  $k_H^{(0)}$ , as a function of the exponent  $\alpha$  of the Kuhn-Mark-Houwink equation. The full lines represent the results from earlier measurements within the higher molecular weight region for solutions of PIB and polystyrene (PS) in different solvents. The full circles give the data calculated for the system IO/PIB from Figure 9 for  $M \geq 26$  kg/mol, and the empty ones for  $M \leq 26$  kg/mol.

thermodynamic pair interaction, the  $k_H^{(1)}$  and  $k_H^{(0)}$  values concerning the higher molecular weight region agrees reasonably well with the hitherto existing information; in the low molecular weight regime these parameters assume values that deviate even more strongly from the normal behavior than in the case of  $\chi$  as is depicted in Figure 10. The effect for the opening of inner contacts is reduced from ca. -0.1 to -7.2 and that for outer contacts increases from ca. 0.5 to 1.8.

**Situation with Short Chains.** The observation of particular effects in the region of low molecular weights is by no means new and has already been discussed on the basis of the excluded-volume theory.

Orofino and Flory<sup>12</sup> have calculated the excluded volume  $u$  and consequently  $A_2 [ = N_A u / (2M_2) ]$  by means of the free energy arising from the increased segment-segment interaction when two polymer molecules immersed in solvent, and initially far apart, are brought together. This approach, which does not distinguish between inter- and intramolecular contacts, takes account for triple contacts between segments and demonstrates that their influence may become appreciable for low molecular weights and poor solvents. Pouchlý and Patterson<sup>13</sup> have pointed out that such contacts between three segments may be of particular importance in the case of mixed solvents for the values of the unperturbed dimension obtained by means of extrapolation procedures. For low molecular weight polymers, Huber and Stockmayer<sup>14</sup> have observed deviations of  $A_2$  from the predictions of two-parameter theories and attributed them to local chain stiffness and, in the case of  $\theta$  conditions, to three-body interactions.

Recently, an overview entitled "Some Unsolved Problems on Dilute Polymer Solutions" was given by Fujita.<sup>15</sup> In the paragraph dealing with  $A_2$ , the author demonstrates that our knowledge in this area still leaves much to be desired. A further item can be added to this list of experimental observations that are in disagreement with existing theories, namely, the dependence  $A_2(M)$  in the vicinity of exothermal  $\theta$  conditions,<sup>1</sup> where  $A_2$  becomes larger as  $M$  is increased.

In fact, it was the above discrepancy that led to the present concept of intramolecular contributions to the second osmotic virial coefficient in addition to the (normally prevailing) intermolecular ones. Further

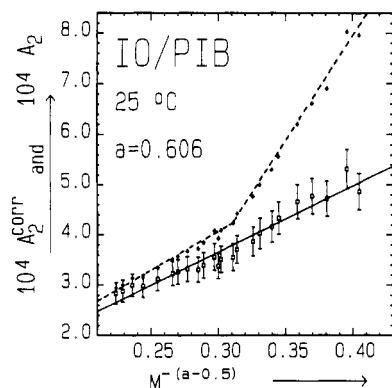


**Figure 11.** Evaluation of the corrected second osmotic virial coefficients (eq 12, with  $\chi_1^+ = 0$ ) according to eq 4. The bars indicate the most probable error of  $A_2$ , which amounts to  $\pm 7.5\%$  with the present measurements. For comparison, the dependence resulting with the original  $A_2$  values (dashed line) is also shown.

theoretical implications of this concept, in particular with respect to the dependence of intrinsic viscosities on solvent quality, will be discussed in a separate paper.<sup>17</sup> The following section is confined to the question how the present approach of different inter- and intramolecular interactions, if applied analogously to the ideas of Orofino and Flory,<sup>12</sup> can explain the discontinuities shown in Figures 7 and 9.

The starting point of these considerations is the fact that the osmotic virial coefficients refer to polymer *molecules* (since they measure the *excess* Gibbs energy of the solvent), in contrast to the Flory–Huggins interaction parameter  $\chi$ , which refers to polymer *segments* (since it measures the *residual* Gibbs energy of the solvent). The dependence of the chemical potential of the solvent on  $\varphi$ , the volume fraction of polymer, is formulated in eq 8 in terms of the osmotic virial coefficients and in eq 9 in terms of  $\chi$

$$G_1/(RT) = V_1\rho M^{-1}\varphi - A_2V_1\rho^2\varphi^2 - A_3V_1\rho^3\varphi^3 \dots \quad (8)$$

$$G_1/(RT) =$$

$$V_1\rho M^{-1}\varphi - ((1/2) - \chi_0)\varphi^2 - ((1/3) - \chi_1)\varphi^3 \dots \quad (9)$$

where  $\chi$  is treated concentration dependent in order to cover all observed functions  $G_1(\varphi)$ .

With the present experiments  $\varphi$  was in all cases kept low enough to remain within the region of pair interaction between polymer molecules; i.e., the third term in eq 8 can always be neglected. With eq 9, however, the situation is different. The reason is that even if triplets of polymer *molecules* are practically absent, this may not be true for triplets of polymer *segments*: As the polymer chains become shorter, the volume fraction  $\varphi_0$  of segments within the equivalent sphere of an isolated polymer molecule increases distinctly, since  $\varphi_0 = 1/([\eta]\rho)$ , and the probability of intramolecular intersegmental contacts rises. This situation leads to the formation of triplets of segments as a second polymer molecule starts to overlap, even if the solution is so dilute that triplets of polymer molecules play no role at all. In order to account for this fact, eq 9 should be rewritten as

$$G_1/(RT) = V_1\rho M^{-1}\varphi - ((1/2) - \chi_0)\varphi^2 - ((1/3) - \chi_1^+)\varphi_0\varphi^2 \dots \quad (10)$$

This relation results from the inhomogeneous space filling of polymer segments in the dilute case. Since the probability for the formation of pairs of contacting segments belonging to *different* molecules is proportional

to  $\varphi^2$  and there are only two molecules overlapping, the probability for the occurrence of a triple of contacting segments is proportional to  $\varphi^3\varphi_0$ . (Two segments belong to chain A and one to chain B, or vice versa.)

In eq 10 the third term can be neglected as compared with the second, as long as  $\varphi_0$  remains small enough, i.e., only in the case of sufficiently large  $[\eta]$  values. Independent of size of the polymer molecules the following expression, obtained from the comparison of the eqs 8 and 10, should, however, hold true:

$$A_2 = [((1/2) - \chi_0) + ((1/3) - \chi_1^+)\varphi_0]/(V_1\rho^2) \quad (11)$$

Equation 11 implies that the measured  $A_2$  values contain a contribution, in addition to the molecular weight dependence expressed by eqs 4–6, which depends on  $M$  via  $\varphi_0$  and therefore becomes noticeable in the region of short chains. In order to check the validity of the present considerations, the measured  $A_2$  values were corrected according to

$$A_2^{\text{corr}} = A_2 - ((1/3) - \chi_1^+)\varphi_0/(V_1\rho^2) \quad (12)$$

and evaluated on the basis of eq 4 as shown in Figure 11. In view of the comparatively small influence of  $\chi_1^+$  and of the experimental errors in the determination of  $A_2$ ,  $\chi_1^+$  was set equal to zero, even if negative values for this parameter would improve the linearity.

From the slope and the intercept of the relation shown in Figure 11 one obtains for the entire region of molecular weights  $\chi^{(1)} = 0.421$  (instead of 0.412 and 0.357 for high and low  $M$ , respectively) and  $\chi^{(0)} = 0.587$  (instead of 0.596 and 0.883). These values are in good agreement with all previous results, which stem exclusively from measurement with high molecular weight polyisobutylene, as can be seen from the solid line drawn in Figure 8 for this polymer.

The particular effects encountered with short chains in the case of the Huggins coefficients  $k_H$  will not be discussed here, since the precision and the number of measurements are considerably less than with  $A_2$ . Qualitatively it can, however, be stated that a similar discontinuity has to be expected in view of the thermodynamic influences that lead to relations  $k_H(A_2)$  (cf. for instance ref 16).

## References and Notes

- (1) Wolf, B. A.; Adam, H. J. *J. Chem. Phys.* **1981**, *75*, 4121.
- (2) Wolf, B. A. *Macromolecules* **1985**, *18*, 2474.
- (3) Gundert, F.; Wolf, B. A. *Makromol. Chem.* **1986**, *187*, 2969.
- (4) Gundert, F.; Wolf, B. A. *J. Chem. Phys.* **1987**, *87*, 6156.
- (5) Geerissen, H.; Roos, J.; Schützeichel, P.; Wolf, B. A. *J. Appl. Polym. Sci.* **1987**, *34*, 271.
- (6) Geerissen, H.; Roos, J.; Schützeichel, P.; Wolf, B. A. *J. Appl. Polym. Sci.* **1987**, *34*, 287.
- (7) Brandrup, J.; Immergut, E. H. *Polymer Handbook*, 2nd ed.; Wiley-Interscience: New York, 1975; p IV-273.
- (8) Bodmann, O. *Chem. Ing. Tech.* **1957**, *29*, 468.
- (9) Huglin, M. B. *Light Scattering from Polymer Solutions*; Academic Press: London, New York, 1972.
- (10) Stockmayer, W. H.; Fixman, M. *J. Polym. Sci., Part C* **1963**, *1*, 137.
- (11) Berry, G. C. *J. Chem. Phys.* **1967**, *46*, 1338.
- (12) Orofino, T. A.; Flory, P. J. *J. Chem. Phys.* **1957**, *26*, 1067.
- (13) Pouchlý, J.; Patterson, D. *Macromolecules* **1973**, *6*, 465.
- (14) Huber, K.; Stockmayer, W. H. *Macromolecules* **1987**, *20*, 1400.
- (15) Fujita, H. *Macromolecules* **1988**, *21*, 179 and literature cited therein.
- (16) Bohdanecký, M.; Kovář, *Viscosity of Polymer Solutions*, *Polymer Science Library* 2; Elsevier: Amsterdam, 1982.
- (17) Wolf, B. A. *J. Chem. Phys.*, submitted.

**Registry No.** Isooctane, 540-84-1; polyisobutylene, 9003-27-4.